Giant-moment clusters in paramagnetic and weakly ferromagnetic Pd-Ni alloys

T. D. Cheung, J. S. Kouvel, and J. W. Garland
Department of Physics, University of Illinois at Chicago Circle, Chicago, Illinois 60680
(Received 19 August 1980)

A series of Pd-Ni alloys, of Ni concentrations up through the critical value (~2.5 at.%) for ferromagnetism, was studied by detailed magnetization measurements from 2.4 to 50 K in fields up to 56 kOe. The paramagnetic susceptibilities and high-field magnetizations are both found to consist of two components arising from stable magnetic clusters and locally enhanced Pauli paramagnetism. The magnetic clusters are shown to be nucleated by groups of three or more nearest-neighbor Ni atoms, as reported earlier, and also by nearest-neighbor Ni pairs that have other Ni pairs (and/or Ni singles) in close proximity. Both types of clusters have giant moments (~17 and ~$12\mu_B$, respectively) and anomalously low spins (2 and 1, respectively), suggesting that the large induced polarization of the Pd atoms around the cluster nuclei has no independent degrees of freedom. Since the fraction of Ni pairs that nucleates magnetic clusters increases rapidly above ~2 at.% Ni and does not contribute significantly to the locally enhanced susceptibility, this susceptibility component has a broad finite peak near the critical concentration. Thus, the onset of ferromagnetism does not derive from any critical exchange enhancement but from a percolation among the interacting clusters.

I. INTRODUCTION

It is well known that, unlike iron or cobalt, nickel as an isolated impurity atom does not form a stable magnetic moment in a nonmagnetic metal host. Even in the most auspicious case, when the metal host is palladium, isolated nickel atoms simply contribute a large and nearly temperature-independent susceptibility arising from local exchange enhancement.[1] However, more recent magnetic measurements in Grenoble[2,3] and in our laboratory[4] have shown that when a Ni atom in Pd has two or more Ni nearest neighbors, it forms a stable magnetic cluster, whose enormous moment [~$18\mu_B$ (Ref. 4)] indicates that it also contains the exchange-induced polarization of many neighboring Pd atoms. Thus, the origin of giant moments in *Pd*Ni is quite similar to that in *Pd*Fe and *Pd*Co, with each group of three or more nearest-neighbor Ni atoms playing a nucleating role analogous to that of a single Fe or Co impurity atom.

From their results, Sain and Kouvel[4] also deduced that the effective spin of a giant-moment cluster in *Pd*Ni is remarkably small (~2), which differs from the larger values (between 5 and 8) obtained by Chouteau[3] but which resembles the low spin values derived from specific-heat data[5,6] on *Pd*Fe and *Pd*Co. Moreover, for the average moment per cluster, Sain and Kouvel found no measurable deviation from a value of ~$18\mu_B$ (or from a spin value of ~2) in alloys of up to ~1.8 at.% Ni, although they did observe that for a 1.95 at.% Ni alloy these values are no longer applicable within a simple interpretation. Chouteau, on the other hand, obtained giant-moment values that increased from ~$10\mu_B$ for a 1.29 at.% Ni alloy to ~$16\mu_B$ for 1.65 at.% Ni, the increase being ascribed to the induced moments of isolated Ni atoms and nearest-neighbor Ni pairs that lie within the polarization radius of a magnetic cluster. A more consistent picture is clearly needed for the magnetic properties of a broader composition range of Pd-Ni alloys.

In this paper, we will present the results of magnetic measurements on Pd-Ni alloys of Ni concentrations that extend up to and somewhat beyond the critical value [~2.5 at.% (Refs. 7 and 8)] for the onset of ferromagnetism, where neutron scattering experiments have already given evidence of magnetic clusters.[9] From the analysis of our results (and those of Sain and Kouvel[4] for lower Ni concentrations), we will deduce the principal local-environment criteria for stable magnetic-moment formation that are consistently pertinent in both the paramagnetic and weakly ferromagnetic regimes.

II. EXPERIMENTAL TECHNIQUES AND RESULTS

Our Pd-Ni alloy samples, ranging in Ni concentration from 2.1 to 3.0 at.%, were cut as cylinders (3 mm in diameter, 6 mm long) from buttons made by arc melting 99.995% pure metals under argon, and were then annealed for 5 d at 1000 °C and water quenched. These procedures and the batches of pure metals were identical to those used earlier[4] for the preparation of alloy samples of lower Ni concentration. The samples, like the earlier ones, contained a

superparamagnetic (presumably Fe) impurity of ~20 ppm, whose very small contributions to the measured properties were subtracted out, as indicated later in Table I. The magnetizations of the samples were measured with a temperature-controlled vibrating-sample magnetometer between 2.4 and 50 K in fields from 20 Oe up to 56 kOe.

The magnetization versus field (σ vs H) curves we obtained at 2.4 K are displayed in Fig. 1, together with those of Sain and Kouvel[4] for alloys of 1.3–1.95 at.% Ni and for pure Pd. Figure 2 displays our results and those of the earlier work for the inverse initial susceptibility (χ_0^{-1}) as a function of temperature (T). In both cases, our measurements provide very smooth extensions of the earlier results up through the critical concentration (2.5 at.% Ni), for which it is seen that χ_0^{-1} approaches zero at 0 K. The ferromagnetism of the 2.8 and 3.0 at.% Ni alloys is evidenced by their nonzero spontaneous magnetizations and by the positive intercepts of χ_0^{-1} with the T axis, indicating Curie temperatures of ~6 and ~10 K, respectively.

Furthermore, the χ_0^{-1} vs T curves in Fig. 2 for the ferromagnetic and nearly ferromagnetic alloys are seen to develop a positive (concave-upwards) curvature at low temperatures, which is typical of magnetic short-range ordering, whereas at higher temperatures they exhibit a distinctly negative curvature. This

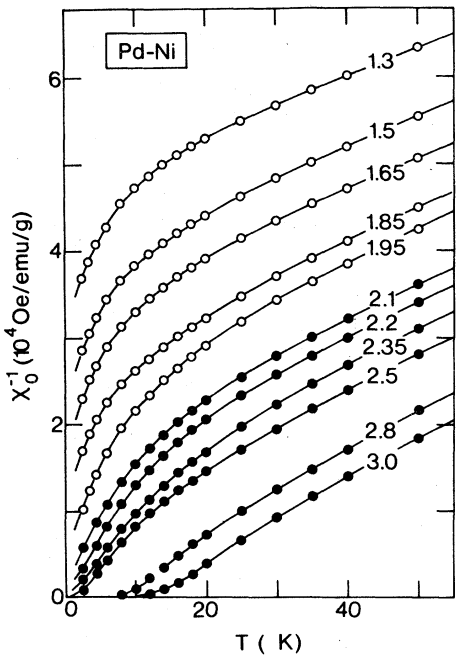

FIG. 2. Inverse initial susceptibility (χ_0^{-1}) vs temperature (T) for various Pd-Ni alloys (designated by at.% Ni). Closed circles from present work; open circles from Ref. 4.

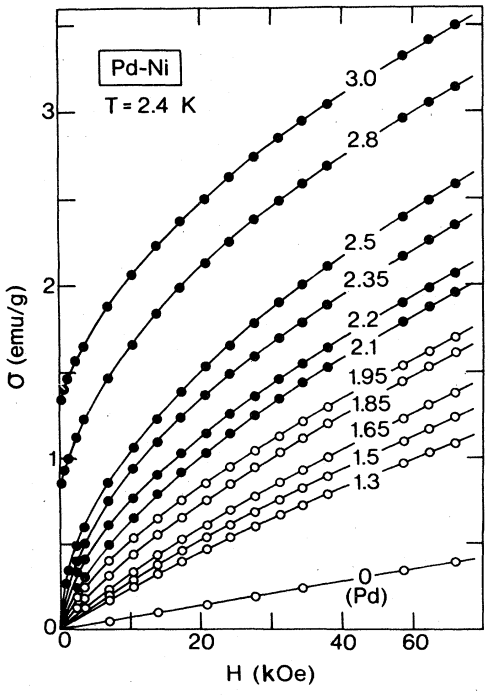

FIG. 1. Magnetization (σ) vs field (H) at 2.4 K for various Pd-Ni alloys (designated by at.% Ni) and for pure Pd. Closed circles from present work; open circles from Ref. 4.

negative curvature, which exists at all temperatures for the more weakly magnetic alloys ($\leq$1.95 at.% Ni), was shown earlier[4] to be consistent with the coexistence of a Curie-Weiss-like susceptibility component contributed by superparamagnetic clusters, and a relatively temperature-independent susceptibility component derived from locally enhanced Pauli paramagnetism. Hence, in Sec. III, the analysis of our results for the more strongly magnetic alloys will start with a similar component separation of the measured paramagnetic susceptibility and, again following the earlier work,[4] with an analogous separation of the low-temperature magnetization versus field curves in Fig. 1.

III. DATA ANALYSIS AND DISCUSSION

Since the Curie-Weiss-like component of the susceptibility becomes increasingly dominant with increasing Ni concentration, as evidenced in Fig. 2, it becomes correspondingly difficult to separate out the other susceptibility component (χ') whose weak temperature dependence is to be determined from the separation. Fortunately, for the alloys of low ($\leq$1.95) at.% Ni, where such a separation was achieved quite easily, it was found that although χ' varies with alloy composition its relative changes with

temperature remain essentially the same.[4] Hence, for the alloys of higher Ni concentration, after assuming that their initial susceptibilities can be similarly resolved into a Curie-Weiss-like cluster component (χ_{cl}) and an exchange-enhanced component (χ'), i.e.,

$$\chi_0 = \chi_{cl} + \chi', \quad \chi_{cl} = C_{cl}/(T-\theta) \ , \tag{1}$$

we further assumed that χ' has the same relative temperature dependence that it has at lower Ni concentrations. Using the χ' vs T curve determined previously for 1.95 at.% Ni,[4] we adjusted the scale of χ' for each alloy so as to attain the most linear variation of $(\chi_0 - \chi')^{-1}$ with temperature. The results thus obtained for χ_{cl}^{-1} vs T are plotted in Fig. 3 and, in each case, the variation is essentially linear except for the positive low-temperature curvature that presumably arises from magnetic short-range ordering. Also displayed in Fig. 3 are the relatively flat χ'^{-1} vs T curves used for this analysis. The extrapolated zero-temperature values of χ', that is $\chi'(0)$, and the values of C_{cl} and θ determined from the slopes and temperature intercepts of the linear portions of χ_{cl}^{-1} vs T are listed in Table I, together with the values obtained earlier for the alloys of lower Ni concentration.[4]

For the latter alloys, it was also found that the $\chi'(0)$ values deduced from the low-field susceptibility differ very little from the high-field slopes of the low-temperature σ vs H curves. It was thus concluded that χ' is nearly field-independent up to ~ 50 kOe and that at these high fields the cluster contribution to the magnetization (σ_{cl}) has reached its saturation value, which could then be determined by a simple extrapolation to zero field. However, for the alloys of higher at.% Ni, the σ vs H curves in Fig. 1 are decreasing in slope up to our highest field, which—under the assumption that χ' remains fairly constant—indicates that σ_{cl} has not yet attained saturation. Hence, in order to determine σ_{cl} for these alloys, we adopted a somewhat different tactic. In Fig. 4, we have plotted all our magnetization data at 2.4 K as σ^2 vs H/σ. These Arrott plots are very anomalous in their strong positive curvature, which in itself suggests that more than one process is contributing to the magnetization. We therefore assumed by analogy with Eq. (1) that the measured low-temperature magnetization consists of two components as follows:

$$\sigma = \sigma_{cl} + \chi' H \ , \tag{2}$$

where, for each alloy, χ' has the zero-temperature

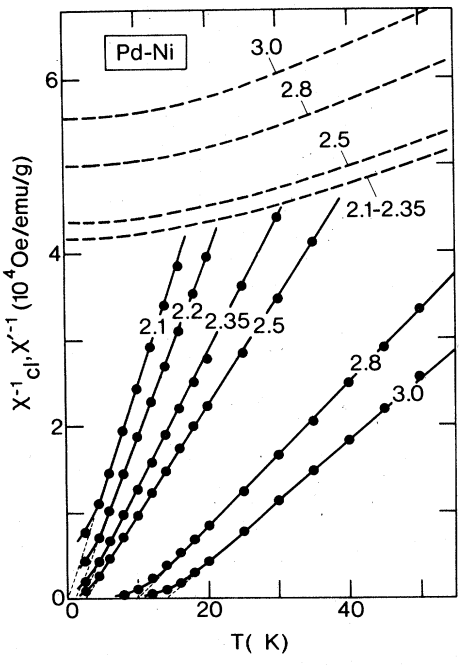

FIG. 3. Temperature dependence of χ_{cl}^{-1} (solid curves) and of χ'^{-1} (dashed curves) for various Pd-Ni alloys (designated by at.% Ni), where $\chi_{cl} + \chi' = \chi_0$, the measured initial susceptibility.

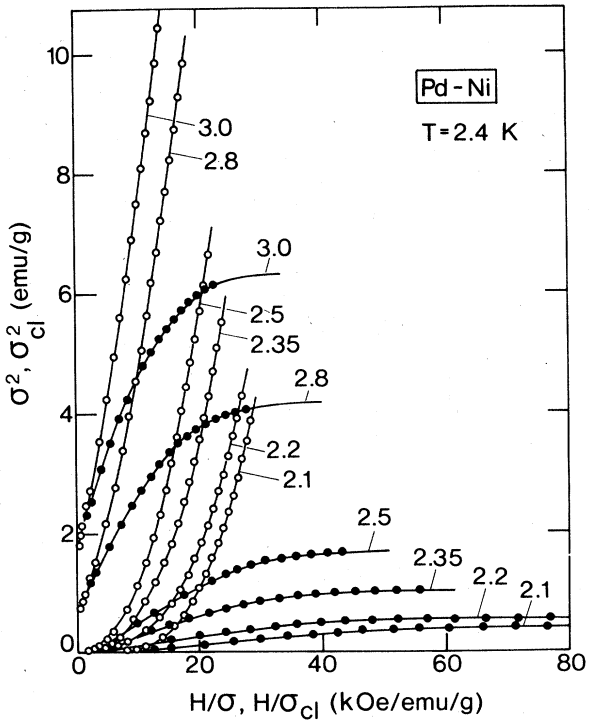

FIG. 4. Arrott plots of σ^2 vs H/σ (open circles) and σ_{cl}^2 vs H/σ_{cl} (closed circles) at 2.4 K for various Pd-Ni alloys (designated by at.% Ni).

(and field-independent) value $\chi'(0)$ listed in Table I, as determined from χ_0. After subtracting $\chi' H$ from each measured σ (at 2.4 K) to obtain σ_{cl}, we proceeded to calculate the revised Arrott plots of σ_{cl}^2 vs H/σ_{cl} displayed in Fig. 4. In contrast to the original Arrott plots, the new plots show a normal negative curvature which eventually, at our highest fields, develops into an approach to saturation. The saturation values of σ_{cl} readily determined from these plots are listed in Table I, together with those for the alloys of lower at.% Ni.[4]

Our numerical results for the saturation magnetization (σ_{cl}) and Curie-Weiss constant (C_{cl}) that derive from magnetic clusters in Pd-Ni, as well as the earlier results,[4] are plotted against Ni concentration in Fig. 5. Both σ_{cl} and C_{cl} are seen to vary smoothly and monotonically through the critical concentration for ferromagnetism, which the Arrott plots in Fig. 4 confirm to be ~ 2.5 at.% Ni. Also plotted in Fig. 5 (and listed in Table I) are σ_{3+} and C_{3+}, the saturation magnetization and Curie-Weiss constant calculated for magnetic clusters nucleated by groups of three or more nearest-neighbor Ni atoms (whose statistical concentrations[10] c_{3+} are also listed in Table I); the average magnetic moment (μ_{3+}) and spin (S_{3+}) per cluster are taken to be $17\mu_B$ and 2, respectively. Calculations on essentially this basis were found by Sain and Kouvel[4] to give excellent agreement with the σ_{cl} and C_{cl} values deduced for alloys of up to 1.85 at.% Ni, as is evident in Fig. 5 and Table I. This contrasts with Chouteau's results[3] for about the same composition range, where much larger S_{3+} values were invoked and μ_{3+} was considered to grow with increasing Ni concentration. However, Sain and Kouvel did

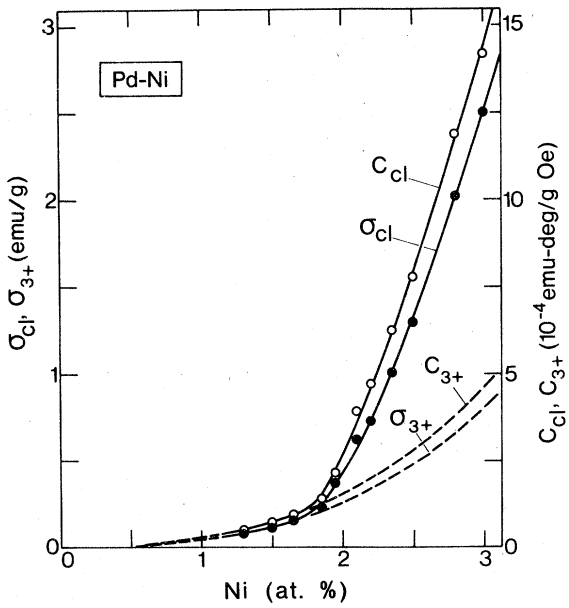

FIG. 5. Experimental values of σ_{cl} and C_{cl} (closed and open circles, respectively) and calculated values of σ_{3+} and C_{3+} (dashed curves) vs Pd-Ni alloy composition.

observe that for a 1.95 at.% Ni alloy the experimentally derived σ_{cl} and C_{cl} were significantly larger than the calculated σ_{3+} and C_{3+}; Fig. 5 shows that this discrepancy becomes even more pronounced at higher Ni concentration.

In order to study this discrepancy, we have plotted

TABLE I. Magnetic and concentration parameters for Pd-Ni alloys.

Alloy (at.% Ni)	$\chi'(0)$ (10^{-6} emu/g Oe)	θ (K)	C_{cl}[a] (10^{-6} emu K/g Oe)	C_{3+}	σ_{cl}[a] (emu/g)	σ_{3+}	c_1[b] (10^{-5})	c_2[b] (10^{-6})	c_{3+}[b] (10^{-7})
1.3[c]	17.9	−2	48	47	0.080	0.082	1111	801	914
1.5[c]	20.2	−2	67	70	0.117	0.123	1251	1028	1367
1.65[c]	22.3	−2	92	91	0.155	0.160	1351	1211	1779
1.85[c]	24.5	−2	137	125	0.232	0.219	1479	1467	2440
1.95[c]	23.8	0	214	145	0.374	0.253	1540	1601	2817
2.1	24	0	397	174	0.63	0.30	1628	1806	3392
2.2	24	1	472	200	0.73	0.35	1685	1946	3906
2.35	24	2	624	239	1.01	0.42	1767	2160	4655
2.5	23	3	777	280	1.30	0.49	1845	2377	5455
2.8	20	10	1189	379	2.02	0.66	1991	2821	7382
3.0	18	14	1420	453	2.50	0.79	2082	3121	8825

[a] C_{cl} and σ_{cl} were corrected for 20-ppm Fe impurity by subtracting 9×10^{-6} emu K/g Oe and 0.011 emu/g, respectively, from the experimental values.

[b] See Ref. 10.

[c] Parameters for these alloys were originally reported in Ref. 4.

$C_{cl}-C_{3+}$ vs $\sigma_{cl}-\sigma_{3+}$ in Fig. 6 for each of our alloys, and we note that the variation is smooth and extends almost linearly to the origin. Let us first consider the possibility that these two difference quantities derive from an enlargement of the cluster moment due to the induced polarization of single Ni atoms and nearest-neighbor Ni pairs close to a Ni-triad cluster core, as proposed by Chouteau.[3] If the nearest-neighbor Ni triad (or larger group) constituting the cluster core were surrounded only by polarized Pd atoms, the saturation magnetization and Curie-Weiss constant associated with the clusters would be expressible as

$$\sigma_{3+}=Nc_{3+}\mu_{3+}, \quad C_{3+}=Nc_{3+}\mu_{3+}^2(S_{3+}+1)/3kS_{3+} \ , \tag{3}$$

where N is the number of atoms per gram and k is the Boltzmann constant. It was via these expressions, in fact, that $\mu_{3+}=17\mu_B$ and $S_{3+}=2$ were deduced for Ni concentrations up to 1.85 at.%. However, if we allow the cluster moment to vary as $\mu_{3+}(1+\alpha)$, where α is the relative contribution from polarized Ni singles and pairs, the cluster magnetization and Curie-Weiss constant become

$$\sigma_{cl}=\sigma_{3+}(1+\alpha), \quad C_{cl}=C_{3+}(1+\alpha)^2 \ ,$$

which combine to give

$$\frac{C_{cl}-C_{3+}}{C_{3+}}=\frac{2(\sigma_{cl}-\sigma_{3+})}{\sigma_{3+}}+\frac{(\sigma_{cl}-\sigma_{3+})^2}{\sigma_{3+}^2} \ . \tag{4}$$

Using this expression and the values of σ_{cl}, σ_{3+}, and C_{3+} in Table I, we calculated $C_{cl}-C_{3+}$ for all our alloys and found their values to be 3 to 4 times as large as the values shown in Fig. 6. The calculated $C_{cl}-C_{3+}$ values (times $\frac{1}{4}$) are plotted in this figure, and it is clear that their variation with $\sigma_{cl}-\sigma_{3+}$ is qualitatively different from that of the directly determined values. Hence, it appears that these difference quantities and their almost linear interdependence do not stem from any appreciable changes of the average moment per Ni-triad cluster with alloy composition.

Alternatively, let us now consider the possibility that, in addition to the Ni-triad clusters, magnetic clusters are also nucleated by some other type of Ni-atom group, whose identity is to be determined. In this case, if the latter clusters are designated by the subscript x, the saturation magnetization and Curie-Weiss constant associated with all the clusters can be expressed additively as

$$\sigma_{cl}=\sigma_{3+}+\sigma_x, \quad C_{cl}=C_{3+}+C_x \ ,$$

where σ_{3+} and C_{3+} are given in Eq. (3) and, analogously,

$$\sigma_x=Nc_x\mu_x, \quad C_x=Nc_x\mu_x^2(S_x+1)/3kS_x \ . \tag{5}$$

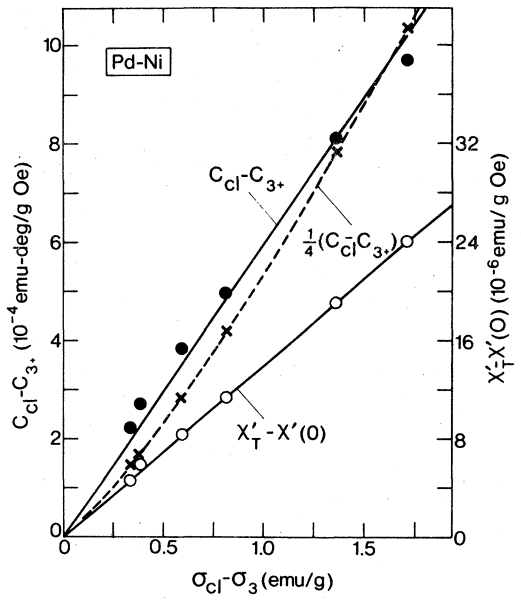

FIG. 6. $C_{cl}-C_{3+}$ and $\chi_T'-\chi'(0)$ vs $\sigma_{cl}-\sigma_{3+}$ (closed and open circles, respectively) for Pd-Ni alloys of 2.1–3.0 at.% Ni. Crosses represent $\frac{1}{4}(C_{cl}-C_{3+})$ vs $\sigma_{cl}-\sigma_{3+}$ calculated from Eq. (4).

Since these expressions give

$$(C_{cl}-C_{3+})/(\sigma_{cl}-\sigma_{3+})=C_x/\sigma_x=\mu_x(S_x+1)/3kS_x \ , \tag{6}$$

where μ_x and S_x are undetermined constants, it follows that $C_{cl}-C_{3+}$ will depend linearly on $\sigma_{cl}-\sigma_{3+}$, in qualitative agreement with the experimentally derived results in Fig. 6. Furthermore, since the straight line that closely approximates these results has a slope of 5.95×10^{-4} deg/Oe, we deduce from Eq. (6) that

$$\mu_x(S_x+1)/S_x=26.6\mu_B \ . \tag{7}$$

To test this possibility further, we will examine it against our results for $\chi'(0)$, the susceptibility component at 0 K that derives from local exchange enhancement (and also includes the enhanced susceptibility of the Pd matrix). For the alloys of ≤ 1.85 at.% Ni, it was found[4] that the values of $\chi'(0)$ could be fitted very closely by the calculated quantity,

$$\chi_T'=(1-c_1-2c_2)\chi_{Pd}'+c_1\chi_1'+c_2\chi_2' \ , \tag{8}$$

where $\chi_{Pd}'=0.069$, $\chi_1'=3.5$, and $\chi_2'=90$ (in 10^{-4} emu/g Oe) are, respectively, the contributions from a Pd atom, an isolated Ni atom, and a nearest-neighbor Ni pair. c_1 and c_2 are the statistical concentrations of the Ni singles and pairs, whose values[10] are listed in Table I. The component terms of χ_T' in Eq. (8), calculated on this basis, are plotted cumulatively as functions of Ni concentration in Fig. 7(a). Also plotted here are the experimental values of $\chi'(0)$ for all

the alloys (including those of Sain and Kouvel[4]) as well as the values obtained by Chouteau[11] for alloys of lower at.% Ni. We note that the experimental $\chi'(0)$ values rise along the calculated χ'_T curve up to ~ 1.8 at.% Ni, but then fall increasingly below this curve at higher Ni concentrations, where they ultimately go through a broad maximum and start to decrease. In fact, the variation of $\chi'(0)$ above ~ 1.8 at.% Ni appears to be such that the Ni-pair contribution ($c_2\chi'_2$) is rapidly disappearing. This suggests that an increasing fraction of the Ni pairs may be forming stable local moments, in which case the concentration of these polarized Ni pairs may be expressed as $[\chi'_T-\chi'(0)]/\chi'_2$. If we proceed to identify these polarized Ni pairs with the Ni-atom groups of concentration c_x, to which we attributed the nucleation of magnetic clusters (other than those nucleated by Ni triads), it follows that:

$$\chi'_T-\chi'(0)=c_x\chi'_2 \ , \tag{9}$$

which, combined with the expression for $\sigma_x(=\sigma_{cl}-\sigma_{3+})$ in Eq. (5), yields

$$[\chi'_T-\chi'(0)]/(\sigma_{cl}-\sigma_{3+})=\chi'_2/N\mu_x \ . \tag{10}$$

Since all the quantities on the right are essentially constant, Eq. (10) expresses a linear relationship between $\chi'_T-\chi'(0)$ and $\sigma_{cl}-\sigma_{3+}$. For comparison, values of $\chi'_T-\chi'(0)$ were taken from Fig. 7(a) for our various alloys and plotted against $\sigma_{cl}-\sigma_{3+}$ in Fig. 6. The plot is seen to fit a straight line extending to the origin and thus conforms to Eq. (10). Equating the slope of this straight-line fit, which is 13.9×10^{-6} Oe^{-1}, with the right-hand side of Eq. (10), where $\chi'_2=90\times10^{-4}$ emu/g Oe and $N=5.7\times10^{21}$ g^{-1}, we obtain

$$\mu_x=12.2\mu_B \ ,$$

which, together with the result in Eq. (7), gives

$$S_x=0.85\approx1 \ .$$

These results for the clusters formed around Ni pairs are not very different from the giant moment ($17\mu_B$) and low spin (2) deduced earlier for the clusters formed around Ni triads. Both these moment values, however, are much larger than the cluster moments of $\sim 4.5\mu_B$ obtained from neutron scattering data on some weakly ferromagnetic Pd-Ni alloys.[9] But as Chouteau[3] has correctly pointed out, the neutron results correspond to integrations over the spatial fluctuations of the local magnetization, which for a high concentration of overlapping ferromagnetic clusters are bound to be smaller than the total moment of an individual cluster.

As we have shown from a simple but consistent interpretation of the linear relationships found among the quantities, $\sigma_{cl}-\sigma_{3+}$, $C_{cl}-C_{3+}$, and $\chi'_T-\chi'(0)$, it can be readily concluded that magnetic clusters in

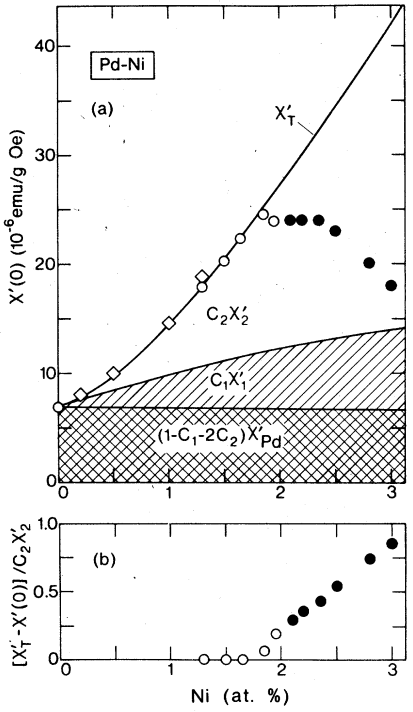

FIG. 7. (a) Experimental $\chi'(0)$ values from present work (closed circles), Ref. 4 (open circles), and Ref. 11 (diamonds) plotted vs Pd-Ni alloy composition and compared with cumulative plot of component terms of χ'_T. (b) Corresponding values of $[\chi'_T-\chi'(0)]/c_2\chi'_2$ vs alloy composition.

Pd-Ni are nucleated not only by nearest-neighbor Ni triads (and larger groups) but also by some fraction of the nearest-neighbor Ni pairs. Furthermore, according to this picture, the fraction of Ni pairs acting as cluster nuclei is c_x/c_2, which from Eq. (9) equals $[\chi'_T-\chi'(0)]/c_2\chi'_2$. Values of this quantity calculated for the different alloys are plotted in Fig. 7(b), where they are seen to rise rapidly from essentially zero when the Ni concentration exceeds ~ 1.8 at.% and reach almost to unity at 3 at.% Ni. Since this variation appears to involve some fairly high power(s) of the Ni concentration, it suggests that the Ni pairs that form magnetic clusters are those in close proximity to other Ni pairs and/or single Ni atoms. The question as to exactly which Ni-atom configurations in a Pd host are capable of stable moment formation, is being examined by us theoretically and will be discussed in a future paper.

A related question arises from our finding that the magnetic clusters in Pd-Ni are all characterized by giant moments and anomalously low values of spin, corresponding to effective g factors of approximately 10. A similar characterization for magnetic clusters in dilute *Pd*Fe and PdCo has been deduced from

specific-heat data.[6,7] In each case, it would appear that the induced polarization of the Pd atoms near a cluster nucleus, which constitutes a major portion of the giant cluster moment, is so tightly coupled to the polarized atom(s) of the nucleus that it has no independent degrees of freedom. The peculiar circumstances that this suggests are presently under theoretical study.

Finally, it should be noted that the results presented here for Pd-Ni have a strong qualitative resemblance to previous analogous results for alloys of Ni with Cu,[12] V,[13] and Rh.[14] In each case, the measured susceptibility has been resolved into a Curie-Weiss-like component (χ_{cl}) ascribable to magnetic clusters which increase rapidly in number as the Ni concentration approaches the critical value for ferromagnetism, and a relatively temperature-independent component (χ') which exhibits a broad finite maximum near the critical concentration. Thus, the onset of ferromagnetism in these systems does not derive from any divergence of χ' but from a percolation among the interacting clusters. Quantitatively, however, there is an important difference between Pd-Ni, where the highly polarizable Pd matrix allows very small groups of neighboring Ni atoms to form stable moments, and the other systems, where the number of neighboring Ni atoms required for stable moment formation is much larger (~ 10) and therefore harder to define exactly. Thus, Pd-Ni offers a situation in which the exact criteria for the formation of magnetic clusters can be deduced experimentally with relative ease, and we have taken advantage of this situation.

ACKNOWLEDGMENT

Support for this work by the NSF under Grant No. DMR78-12777 is gratefully acknowledged.

[1]D. Shaltiel, J. H. Wernick, H. J. Williams, and M. Peter, Phys. Rev. 135, A1346 (1964).

[2]G. Chouteau, R. Tournier, and P. Mollard, J. Phys. (Paris) 35, C4-185 (1974).

[3]G. Chouteau, Physica (Utrecht) B 84, 25 (1976).

[4]D. Sain and J. S. Kouvel, Phys. Rev. B 17, 2257 (1978).

[5]B. W. Veal and J. A. Rayne, Phys. Rev. 135, A442 (1964).

[6]G. J. Nieuwenhuys, B. M. Boerstoel, J. J. Zwart, H. D. Docter, and G. J. Van den Berg, Physica (Utrecht) 62, 278 (1972).

[7]J. E. Van Dam, Ph.D. thesis (University of Leiden, The Netherlands, 1973) (unpublished).

[8]A. P. Murani, A. Tari, and B. R. Coles, J. Phys. F 4, 1769 (1974).

[9]A. T. Aldred, B. D. Rainford, and M. W. Stringfellow, Phys. Rev. Lett. 24, 897 (1970).

[10]For a random binary fcc system of composition $A_xB_y(x+y=1)$, we define c_n as the concentration of groups of n atoms of type A connected by at least one nearest-neighbor bond. As given by R. E. Behringer [J. Chem. Phys. 29, 537 (1958)], $c_1=xy^{12}$, $c_2=6x^2y^{18}$, and $c_3=2x^3y^{22}(4+6y+15y^2)$. By similar counting we have obtained $c_4=x^4y^{24}(2+27y^2+48y^3+96y^4+144y^5+158y^6)$. For the cumulative sum $c_{5+}=c_5+c_6+c_7+\cdots$, we have taken $\frac{1}{5}(x-c_1-c_2-c_3-c_4)$ as a close upper bound for x small. The calculated values of $c_{3+}=c_3+c_4+c_{5+}$ listed in Table I are estimated to be accurate within 0.1% over the range of interest $x \leq 0.03$. The c_{3+} values used in Ref. 4 were derived on a cruder basis and are smaller, resulting in a slight over estimate of the cluster moment μ_{3+}.

[11]G. Chouteau, Ph.D. thesis (University of Grenoble, France, 1973) (unpublished).

[12]J. S. Kouvel and J. B. Comly, Phys. Rev. Lett. 24, 598 (1970).

[13]A. Amamou and B. Loegel, J. Phys. F 3, L79 (1973); A. Amamou, F. Gautier, and B. Loegel, J. Phys. (Paris) 35, C4-217 (1974).

[14]W. C. Muellner and J. S. Kouvel, Phys. Rev. B 11, 4552 (1975).